J. Fluid Mech. (1988), *vol.* 193, *pp.* 243–266
Printed in Great Britain

The nonlinear development of Görtler vortices in growing boundary layers

By PHILIP HALL
Department of Mathematics, Exeter University, North Park Road, Exeter EX4 4QE, UK

(Received 2 December 1986 and in revised form 19 September 1987)

The development of Görtler vortices in boundary layers over curved walls in the nonlinear regime is investigated. The growth of the boundary layer makes a parallel-flow analysis impossible except in the high-wavenumber regime so in general the instability equations must be integrated numerically. Here the spanwise dependence of the basic flow is described using a Fourier series expansion whilst the normal and streamwise variations are taken into account using finite differences. The calculations suggest that a given disturbance imposed at some position along the wall will eventually reach a local equilibrium state essentially independent of the initial conditions. In fact the equilibrium state reached is qualitatively similar to the large-amplitude high-wavenumber solution described asymptotically by Hall (1982*b*). In general it is found that the nonlinear interactions are dominated by a 'mean field' type of interaction between the mean flow and the fundamental. Thus, even though higher harmonics of the fundamental are necessarily generated, most of the disturbance energy is confined to the mean flow correction and the fundamental. A major result of our calculations is the finding that the downstream velocity field develops a strongly inflexional character as the flow moves downstream; the latter result suggests that the major effect of Görtler vortices on boundary layers of practical importance might be to make them highly receptive to rapidly growing Rayleigh modes of instability.

1. Introduction

Our concern is with the effect of nonlinearity on the growth of Taylor–Görtler vortices in developing boundary layers. The presence of such vortices in many flows of practical importance such as those that occur over turbine blades or over laminar-flow aerofoils has recently stimulated much research aimed at understanding their structure in the linear regime. However, the corresponding nonlinear problem has received little attention because of the difficulty in taking care of non-parallel effects.

Some discussion of nonlinear effects was given by Aihara (1976) who derived a nonlinear differential equation to determine the evolution of Görtler vortices. Aihara's calculation ignored non-parallel effects and made other approximations that cannot be formally justified. At high wavenumbers an asymptotic description of the onset of nonlinearity in the Görtler problem was given by Hall (1982*b*) who found that nonlinear effects have a stabilizing influence. Moreover it was shown by Hall that non-parallel effects are crucial in the nonlinear regime. Thus the initial nonlinear development of Görtler vortices is described by a pair of coupled partial differential evolution equations rather than an ordinary differential amplitude equation as is usually the case. In the linear regime it is only in the high wavenumber

limit that non-parallel effects can be accounted for in a 'quasi-parallel' manner, so it would appear that non-parallel effects are important at all wavenumbers in the nonlinear problem. Before discussing the nonlinear problem further it is perhaps worth while for us to review briefly aspects of the linear problem relevant to the present calculation.

In previous investigations Hall (1982*a*, 1983, hereinafter referred to as I, II respectively) discussed the linear Görtler problem. In the first of these papers the wavenumber was taken to be large whilst in the second it was $O(1)$. The calculation of Hall (1982*b*, hereinafter referred to as III) extended I into the nonlinear regime; here we shall make a similar extension to II.

In I, II it was shown that parallel-flow calculations for the Görtler problem are not valid except at high wavenumbers because the streamwise and normal dependences of the vortices cannot be separated. In fact, in the only regime where the instability equations can be reduced to ordinary differential equations, the asymptotic theory of I provides trivially a neutral curve or growth rate at least as accurate as that produced by the parallel-flow theories. It is perhaps necessary at this stage for us to be more precise about what we mean by 'parallel' and 'non-parallel' theories in the context of the Görtler problem. The linear partial differential equations governing the growth of Görtler vortices over a wall of small curvature are given by, for example, Floryan & Saric (1979) or in a much more general context by Gregory, Stuart & Walker (1955). The Görtler number for the flow is held fixed whilst the Reynolds number $R_{\mathrm{E}} \to \infty$, and the terms neglected in the derivation of these equations are formally $O(R_{\mathrm{E}}^{-\frac{1}{2}})$. We refer to these equations as the non-parallel equations for linear Görtler vortices and refer to a 'parallel flow' calculation associated with these equations as being one that neglects some of the terms in these equations without further asymptotic justification. The calculation of II was based on the full equations whereas I used a high-wavenumber approximation to solve the non-parallel equations by a sequence of self-consistent asymptotic approximations. The calculation of Floryan & Saric (1979) at order-one wavenumbers is a parallel-flow approximation because streamwise derivatives acting on disturbance velocities are replaced by constants. Previous parallel-flow theories were given by Görtler (1940), (later corrected numerically by Hämmerlin 1956), who retained only the terms that would be present in the corresponding Taylor–Couette flow calculation, and Smith (1955), who retained many terms associated with the growth of the boundary layer. Other truncations of the instability equations have been solved and the reader is referred to the paper by Herbert (1976) for a detailed review of these calculations.

At $O(1)$ wavenumbers the various parallel-flow theories give quite different results and in the most extreme cases predict instability at zero Görtler number or zero wavenumber. In II it was argued that at $O(1)$ wavenumbers these calculations are necessarily incorrect because their neglect of streamwise derivatives of the disturbance velocity field gives the wrong structure for the disturbance at the edge of the boundary layer. If these terms are retained it was shown that the vortices decay to zero at the edge of the boundary layer at a rate independent of the vortex wavenumber. In fact the linear instability equations are parabolic in the streamwise direction and can therefore be solved numerically by marching downstream from some initial location. A 'local' neutral position can then be defined to be the point where some disturbance flow quantity has a zero rate of change along the wall. This position depends on the location and form of the initial disturbance so that the notion of a unique neutral curve is not tenable for the Görtler problems. However,

at high wavenumbers the numerical calculations of II converged to the unique asymptotic result of I.

Here we shall extend the parallel-flow calculations of II to the nonlinear regime appropriate to disturbances with wavenumber of $O(1)$. At higher wavenumbers the asymptotic high-wavenumber theory of III showed that the nonlinear problem is dominated by a 'mean field' type of interaction rather than one typical of a Stuart–Watson approach. It was shown that the mean flow correction driven by a finite-amplitude vortex ultimately becomes larger than the vortices driving it. At sufficiently large amplitude the mean flow correction described in III would cause the basic state to develop an inflexion point and might therefore make the bounday layer susceptible to rapidly growing Rayleigh instabilities. A primary aim of the calculation presented here is to investigate this possibility at $O(1)$ wavenumbers. Our calculations will also enable linear instability calculations of finite-amplitude Görtler vortices to be ultimately carried out along the lines of the recent calculation of Bennett & Hall (1988). The latter authors were concerned with the corresponding internal fully developed flow between concentric cylinders and showed that even small-amplitude vortices cause a significant destabilization of the undisturbed flow to Tollmien–Schlichting waves.

There is no rational way to reduce the nonlinear non-parallel Görtler problem to a series of ordinary differential equations using the Stuart–Watson method. Hence we shall solve the equations governing finite-amplitude vortices using a numerical method based on the finite-difference formulation of II together with a Fourier decomposition in the spanwise direction. The vortices are assumed to be steady and the equations governing their development are marched downstream from the initial location where the disturbance is imposed. This is done using the implicit scheme of II, together with an iteration procedure to take care of the nonlinear terms which are now present in the calculation. At each downstream location the energy in each Fourier mode can be calculated in order to monitor the development of the instability. We shall see that nonlinear effects prevent the exponential growth of the disturbances predicted by linear theory. Thus, in the limited number of cases we have investigated, we find that nonlinear effects are stabilizing. We shall also see that any given vortex will, sufficiently far downstream, develop a structure consistent with the nonlinear theory of III. The latter result is to be expected since the effective vortex wavenumber increases in the streamwise direction until the asymptotic theory of III applies.

Apart from the arbitrariness associated with the linear problem described in II the nonlinear problem introduces further complications because of the further freedom we have when imposing the initial disturbance. Our calculations are, of course, restricted to a finite number of situations but nevertheless the similarity between the results enables us to make some tentative conclusions about the role of nonlinear effects in the Görtler problem. The procedure adopted in the rest of the paper is as follows: in §2 we formulate the nonlinear instability equations and describe a numerical scheme which can be used to integrate them. In §3 we describe the results we have obtained and use them to draw some conclusions about nonlinear Görtler vortices.

2. Formulation of the instability equations and their solution

Consider the flow of a viscous fluid of kinematic viscosity ν over a wall of curvature $a^{-1}\kappa(x/l)$. Here l and a are typical lengthscales associated with the downstream

development of the flow and the local radius of curvature of the wall. We take $\bar{U}$ to be a typical flow speed and define a Reynolds number Re by

$$Re = \frac{\bar{U}l}{\nu}, \tag{2.1}$$

and consider the limit of $Re \to \infty$ with the Görtler number G, defined by

$$G = \frac{2l}{a} Re^{\frac{1}{2}}, \tag{2.2}$$

held fixed. Let us take (X, Y, Z) to be dimensionless variables in the streamwise, normal and spanwise directions scaled on l, $Re^{-\frac{1}{2}}l$, $Re^{-\frac{1}{2}}l$ respectively. The velocity field is taken to be of the form

$$\boldsymbol{u} = \bar{U}(\bar{u}(X, Y) + U(X, Y, Z), Re^{-\frac{1}{2}}(\bar{v}(X, Y) + V(X, Y, Z)), Re^{-\frac{1}{2}}W(X, Y, Z)), \tag{2.3}$$

where $(\bar{u}(X, Y), \bar{v}(X, Y))$ corresponds to a Blasius boundary layer and (U, V, W) and the corresponding pressure perturbation P are functions of X, Y, Z. Following the procedure outlined in III it is an easy matter to show from the Navier–Stokes equations that, correct to order $Re^{-\frac{1}{2}}$, U, V, W, P satisfy

$$U_X + V_Y + W_Z = 0, \tag{2.4a}$$

$$U_{YY} + U_{ZZ} - V\bar{u}_Y = \bar{u}U_X + U\bar{u}_X + \bar{v}U_Y + Q_1, \tag{2.4b}$$

$$V_{YY} + V_{ZZ} - G\kappa\bar{u}U - P_Y = \bar{u}V_X + U\bar{v}_X + \bar{v}V_Y + V\bar{v}_Y + Q_2, \tag{2.4c}$$

$$W_{YY} + W_{ZZ} - P_Z = \bar{u}W_X + \bar{v}W_Y + Q_3, \tag{2.4d}$$

where Q_1, Q_2, Q_3 are defined by

$$Q_1 = UU_X + VU_Y + WU_Z, \tag{2.5a}$$

$$Q_2 = UV_X + VV_Y + WV_Z + \tfrac{1}{2}G\kappa U^2, \tag{2.5b}$$

$$Q_3 = UW_X + VW_Y + WW_Z. \tag{2.5c}$$

If the nonlinear functions Q_1, Q_2, Q_3 are set equal to zero in the above equations we recover the equations of II. The nonlinear theory of III gives an asymptotic solution of (2.4) valid in the limit of $\partial/\partial z \gg 1$. This limit is physically relevant because it corresponds to the large-X state of any initial disturbance imposed on the flow. Thus in our numerical calculations we expect to recover qualitatively the results of III sufficiently far downstream from where the initial disturbance is introduced.

In order to reduce (2.4) to a form more suitable for computation we can eliminate P and W from the linear terms in (2.4 b, c, d) to give

$$\left\{\bar{u}_{XYY} + \frac{\partial^4}{\partial Z^4} - \bar{v}_Y \frac{\partial}{\partial Z^2}\right\} V + \bar{v}_X U_{YY} + \left\{\bar{u}_{XXY} - \bar{v}_X \frac{\partial^2}{\partial Z^2} - \kappa G\bar{u}\frac{\partial^2}{\partial Z^2}\right\} U$$
$$+ \left\{\bar{u}_{YY} - \bar{u}\frac{\partial^2}{\partial Y^2} - \bar{u}\frac{\partial^2}{\partial Z^2}\right\} V_X + 2\left\{\bar{u}_{XY} + \bar{u}_X \frac{\partial}{\partial Y}\right\} U_X$$
$$+ V_{YYYY} - \bar{v}V_{YYY} - \left\{\bar{v}_Y - 2\frac{\partial^2}{\partial Z^2}\right\} V_{YY} + \left\{\bar{u}_{XY} - \bar{v}\frac{\partial^2}{\partial Z^2}\right\} V_Y$$
$$= -Q_{1XY} + Q_{2ZZ} - Q_{3YZ}, \tag{2.6}$$

where Q_1, Q_2 and Q_3 are given by (2.5 a, b, c) respectively.

We now write

$$U = U_0 + \sum_{n=1}^{\infty} U_n(X, Y) \cos naZ, \tag{2.7a}$$

$$V = V_0 + \sum_{n=1}^{\infty} V_n(X, Y) \cos naZ, \tag{2.7b}$$

$$W = \sum_{n=1}^{\infty} W_n(X, Y) \sin naZ, \tag{2.7c}$$

where we have anticipated the well-known result that the nonlinear interactions that occur in the Taylor–Görtler problem do not generate a mean flow in the spanwise direction. We further note that in (2.7) we have chosen, without any loss of generality, the origin of Z such that U, V are even in Z whilst W is odd in Z. We then substitute for (U, V, W) from (2.7) into (2.4a) and (2.6) and equate like Fourier coefficients. This procedure shows that the mean flow correction satisfies

$$U_{0YY} - V_0 \bar{u}_Y - \bar{u} U_{0X} - U_0 \bar{u}_X - \bar{v} U_{0Y} = U_0 U_{0X} + V_0 U_{0Y} + F_0, \tag{2.8}$$

where

$$F_0 = \frac{1}{2} \sum_{m=1}^{\infty} \{V_m U_{mY} - U_m V_{mY} - 2maU_m W_m\},$$

and V_0 is determined by

$$\frac{\partial U_0}{\partial X} + \frac{\partial V_0}{\partial Y} = 0. \tag{2.9}$$

For computational purposes we must of course truncate the infinite sums in (2.7) at some suitably large value for the upper limit. We therefore replace the upper limit in (2.7) by N.

We then find that U_n satisfies

$$\begin{aligned} U_{nYY} - n^2a^2U_n - \bar{\bar{u}} U_{nX} - U_n \bar{\bar{u}}_X - V_n \bar{\bar{u}}_Y - \bar{\bar{v}} U_{nY} \\ = F_n = \sum_{\substack{m=1 \\ N+1}}^{N-1} V_{n-m} U_{mY} - U_{n-m} V_{mY} + maW_{n-m} U_m - maU_{n-m} W_m \\ + \sum_{\substack{m=1 \\ n+N}}^{N-n} V_{n+m} U_{mY} - U_{n+m} V_{mY} - maU_m W_{n+m} - maU_{n+m} W_m \\ + \sum_{\substack{m=n+1 \\ n+N}}^{N} V_{m-n} U_{mY} - U_{m-n} V_{mY} - maW_{m-n} U_m - maU_{m-n} W_m, \end{aligned} \tag{2.10}$$

where $\bar{\bar{u}} = \bar{u} + U_0$ and $\bar{\bar{v}} = \bar{v} + V_0$.

An equation of the same form can be derived from (2.6) by equating the coefficients of $\cos naz$. Suppose that U_0, V_0, U_n, V_n, W_n, for $n = 1, 2, 3, \ldots$ are known at X, we now describe how (2.8) and (2.10) can be stepped forward to $X + \epsilon$. The scheme used is essentially that described in II together with an iteration procedure to take care of the nonlinear terms now present. Thus for example the mean flow equation (2.8) is discretized using finite differences in the X- and Y-directions to give

$$\begin{aligned} \frac{U_0^{n+1\,m+1} - 2U_0^{n\,m+1} + U_0^{n-1\,m+1}}{h^2} - \frac{\bar{u}^{nm}}{\epsilon} \{U_0^{n\,m+1} - U_0^{n\,m}\} - \bar{v}^{nm} \frac{\{V_0^{n+1\,m} - V_0^{n-1\,m}\}}{2h} \\ - U_0^{nm} \bar{u}_X^{nm} - V_0^{nm} \bar{u}_Y^{nm} = \frac{U_0^{nk+1}}{\epsilon} \{U_0^{nk+1} - U_0^{nk}\} + V_0^{nk+1} \frac{\{U_0^{n+1k+1} - U_0^{n-1k+1}\}}{2h} + F_0^{nk+1}. \end{aligned} \tag{2.11}$$

Here indices m, n refer to the grid point $X = X_0 + m\epsilon$, $Y = nh$. The nonlinear terms on the right-hand side of (2.11) are initially evaluated with $k = m-1$ and the resulting tridiagonal system can be solved to give U_0 at $X = X_0 + (m+1)\epsilon$. The equation (2.10) can be stepped forward in a similar manner to give $U_m, m = 1, \ldots, N$ at $X = X_0 + (m+1)\epsilon$. Likewise the V-equation can be stepped forward by solving a pentadiagonal system. At this stage the nonlinear terms can be expressed in terms of the velocity field now calculated at $X = X_0 + (m+1)\epsilon$. The equation can then be solved again for the flow quantities at $X = X_0 + (m+1)\epsilon$ and the iteration procedure continued until the change in $U_0^{n\,m+1}$, $U_1^{n\,m+1}$, etc. is sufficiently small. Thus (2.11) and the corresponding equations for U_m, V_m are effectively solved with $k = m$ by iterating on the nonlinear terms on the right-hand side.

3. Results and discussion

We shall first describe some results obtained in order to verify the numerical scheme used. These calculations were carried out at various values of the parameters of the problem but here we shall concentrate on the case

$$a = 0.2, \quad G = 0.0288, \quad \kappa(X) = \frac{X}{20}. \tag{3.1}$$

This choice for the curvature function κ means that the effective local Görtler number varies like $X^{\frac{5}{2}}$ whilst the local wavenumber varies like $X^{\frac{1}{2}}$. The asymptotic theory of I showed that the neutral curve which can be uniquely defined at high wavenumbers has the Görtler number proportional to the fourth power of the wavenumber. This means, on the basis of linear theory, that a vortex of any wavenumber becomes increasingly unstable when X increases.

The basic state for the configuration (3.1) was disturbed at $X = 55$ by imposing the condition

$$U_1(\eta) = \eta^6 \, \mathrm{e}^{-\eta^2}, \quad V_1(\eta) = 0 \tag{3.2}$$

where $\eta = y/(2x)^{\frac{1}{2}}$ and integrating the linearized equations to $X = 100$. At this stage the disturbance is almost locally neutral stable according to the criterion of II and the linear velocity field, i.e. the fundamental ($n = 1$) mode of (2.7), was given an amplitude A equal to the maximum X-disturbance velocity component. The nonlinear equations were then integrated for $X > 100$ and the local growth rates and energies of the different harmonics were calculated. We defined the energy of the nth harmonic to be

$$E_n = \int_0^\infty \{U_n^2(X, Y) + V_n^2(X, Y) + W_n^2(X, Y)\} \, \mathrm{d}Y, \quad n = 1, 2, \ldots \tag{3.3}$$

and the energy of the mean flow distortion was defined by

$$E_0 = \int_0^\infty \{U_0^2(X, Y)\} \, \mathrm{d}Y. \tag{3.4}$$

Here we have omitted the contribution from V_0 since $V_0 \to V_0(X)$ when $Y \to \infty$. The growth rate $\theta_n(X)$ of the nth mode was defined by

$$\theta_n(X) = \frac{\mathrm{d}E_n}{\mathrm{d}X} E_n^{-1}, \tag{3.5}$$

so that for a parallel boundary layer in the linear regime θ_n would be twice the linear spatial amplification rate.

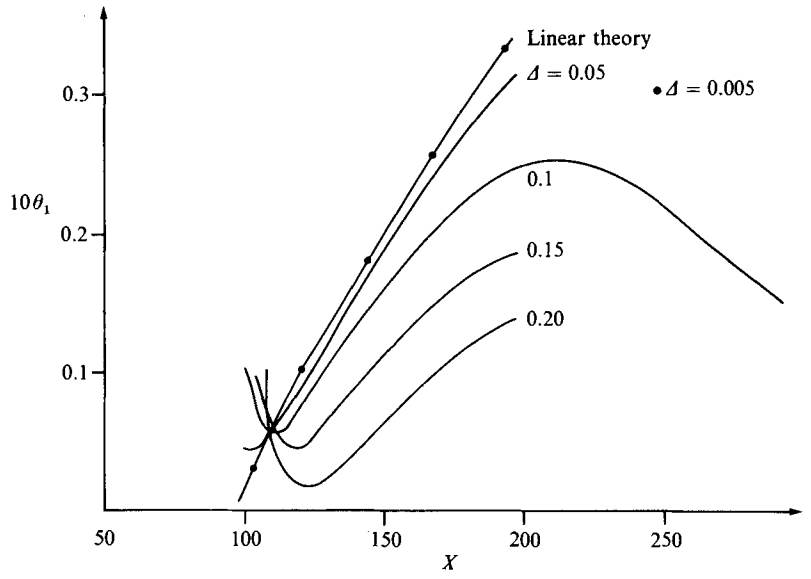

FIGURE 1. The growth rate θ_1 for the wall $\kappa = X/20$, for $\Delta = 0.05$, 0.1, 0.15, 0.2, and $G = 0.0288$, $a = 0.2$.

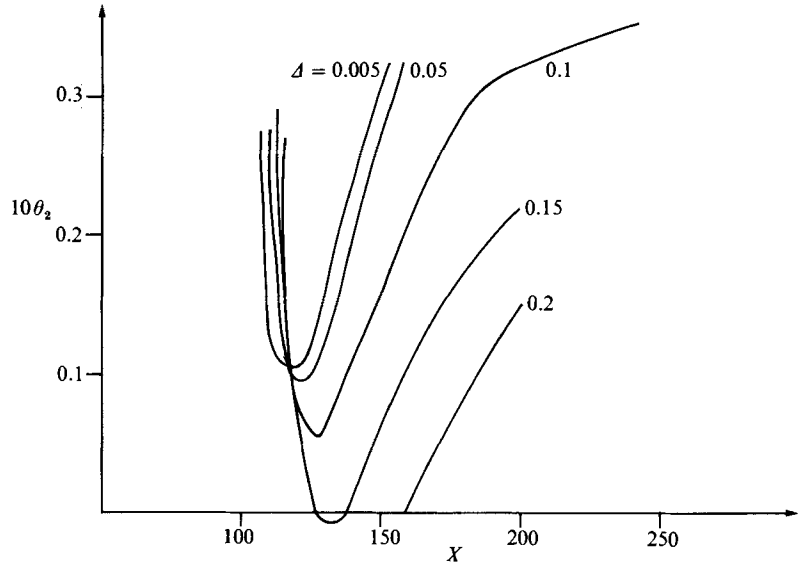

FIGURE 2. The growth rate θ_2 for the wall $\kappa = X/20$, for $\Delta = 0.05$, 0.1, 0.15, 0.2, and $G = 0.0288$, $a = 0.2$.

We know from the non-parallel calculations of I that $\theta_1(X)$ initially depends sensitively on the form and location of the initial disturbance. Here the situation is more complex because we can specify each Fourier mode and the mean flow distribution. In figure 1 we have shown the dependence of θ_1 on X for five different values of Δ, the disturbance flow amplitude. Apart from the fundamental all the Fourier components of the disturbance were set equal to zero at $X = 100$. The calculations shown were carried out with $N = 4$, $\epsilon = 0.025$, $y_\infty = 150$. Similar

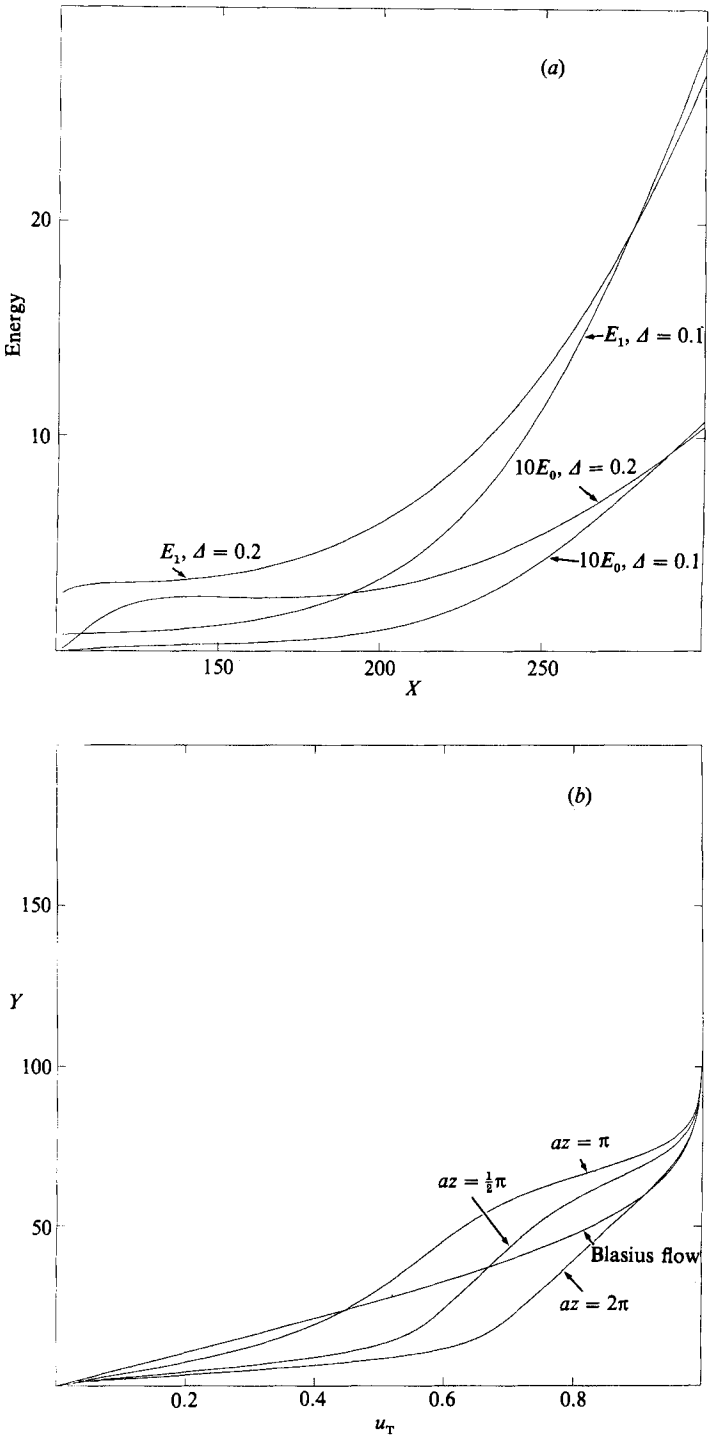

FIGURE 3 (*a*, *b*). For caption see page 253.

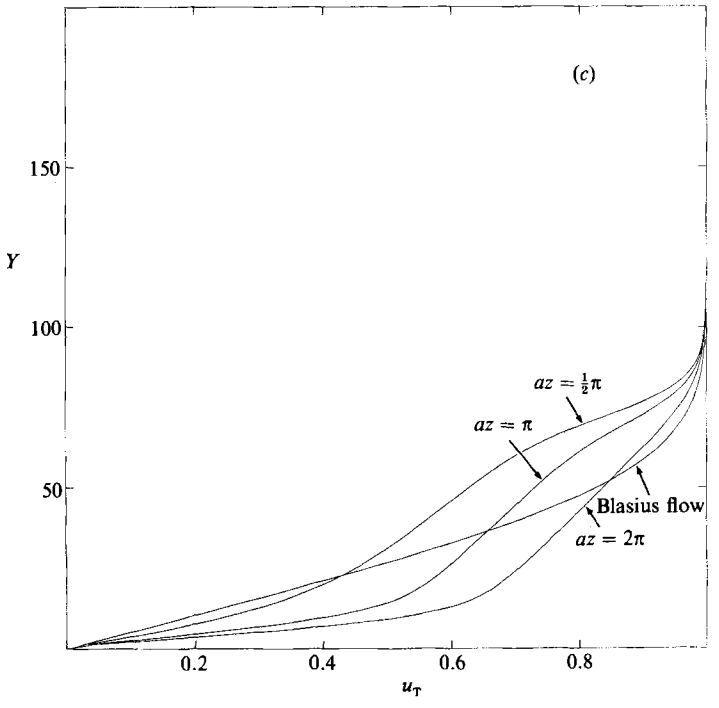

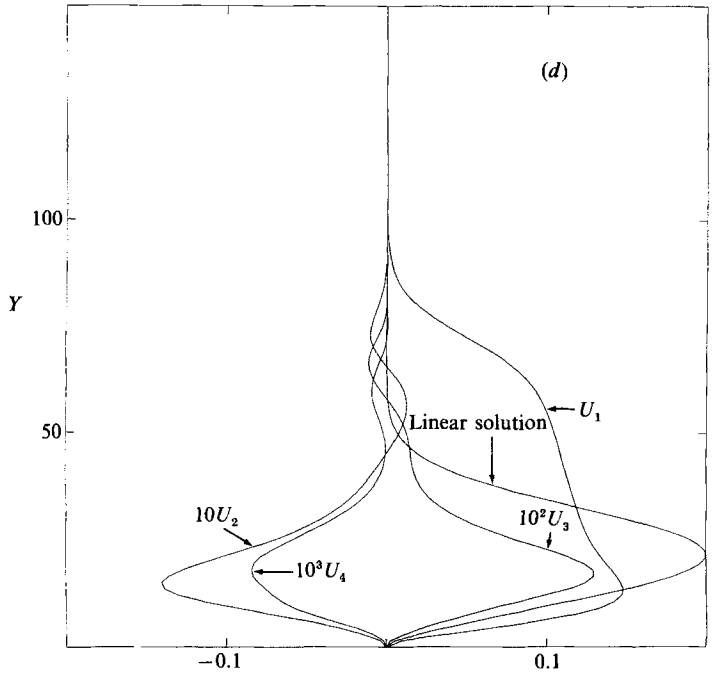

FIGURE 3(*c*, *d*). For caption see page 253.

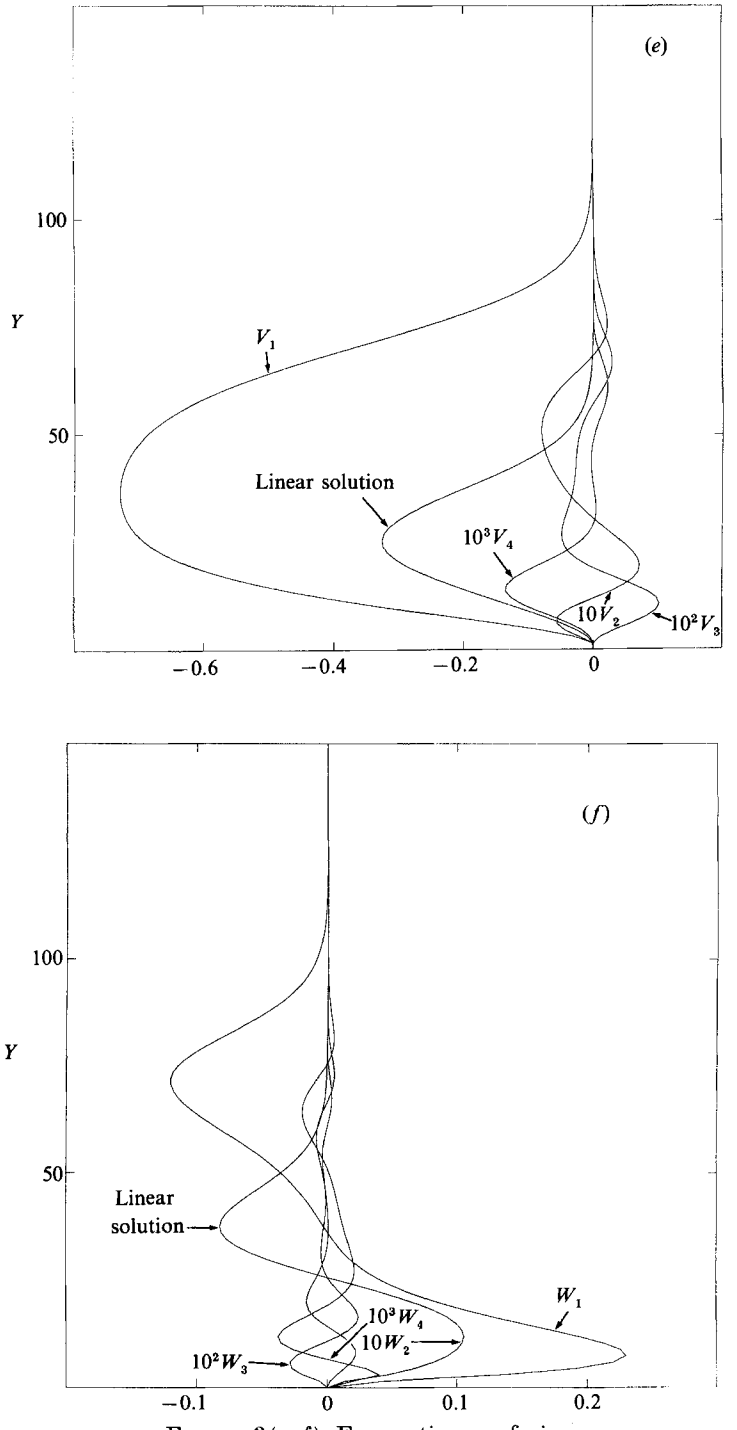

FIGURE 3(*e*, *f*). For caption see facing page.

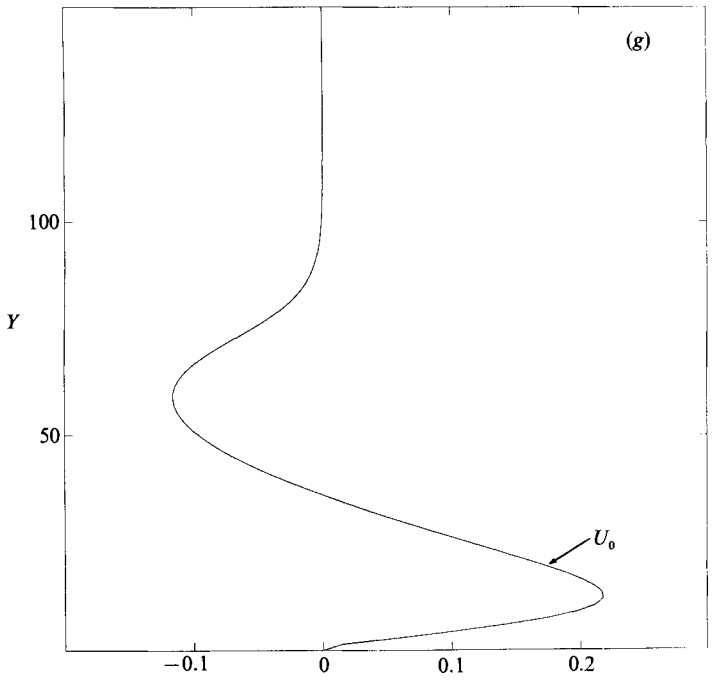

FIGURE 3. (*a*) The energy distributions E_0 and E_1 for $\Delta = 0.1, 0.2$. (*b*) The total streamwise velocity component at different spanwise locations for $X = 300$, $\Delta = 0.1$. (*c*) The total streamwise velocity component at different spanwise locations for $X = 300$, $\Delta = 0.2$. (*d*) The X velocity components at $X = 300$, for $\Delta = 0.2$. (*e*) The Y velocity components at $X = 300$ for $\Delta = 0.2$. (*f*) The Z velocity components at $X = 300$ for $\Delta = 0.2$. (*g*) The mean flow correction at $X = 300$ for $\Delta = 0.2$, all for $\kappa = X/20$, $G = 0.0288$, $a = 0.2$.

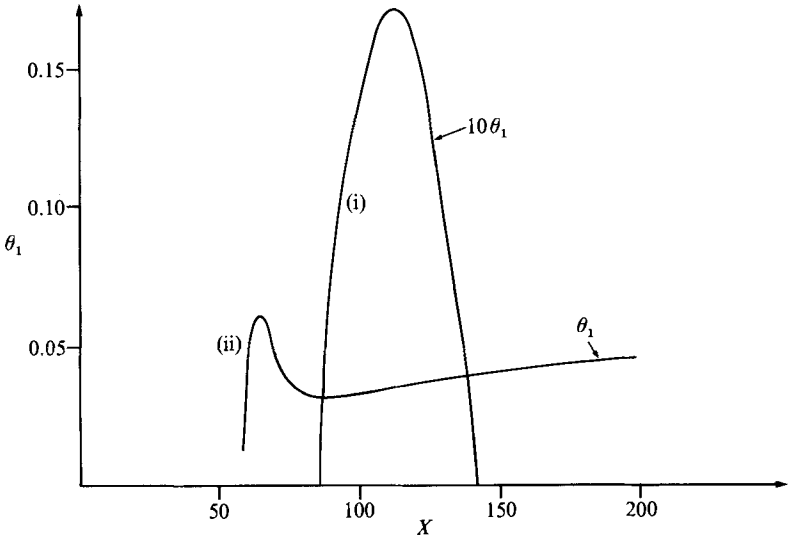

FIGURE 4. The growth rates for the cases (i), (ii) respectively in the linear regime.

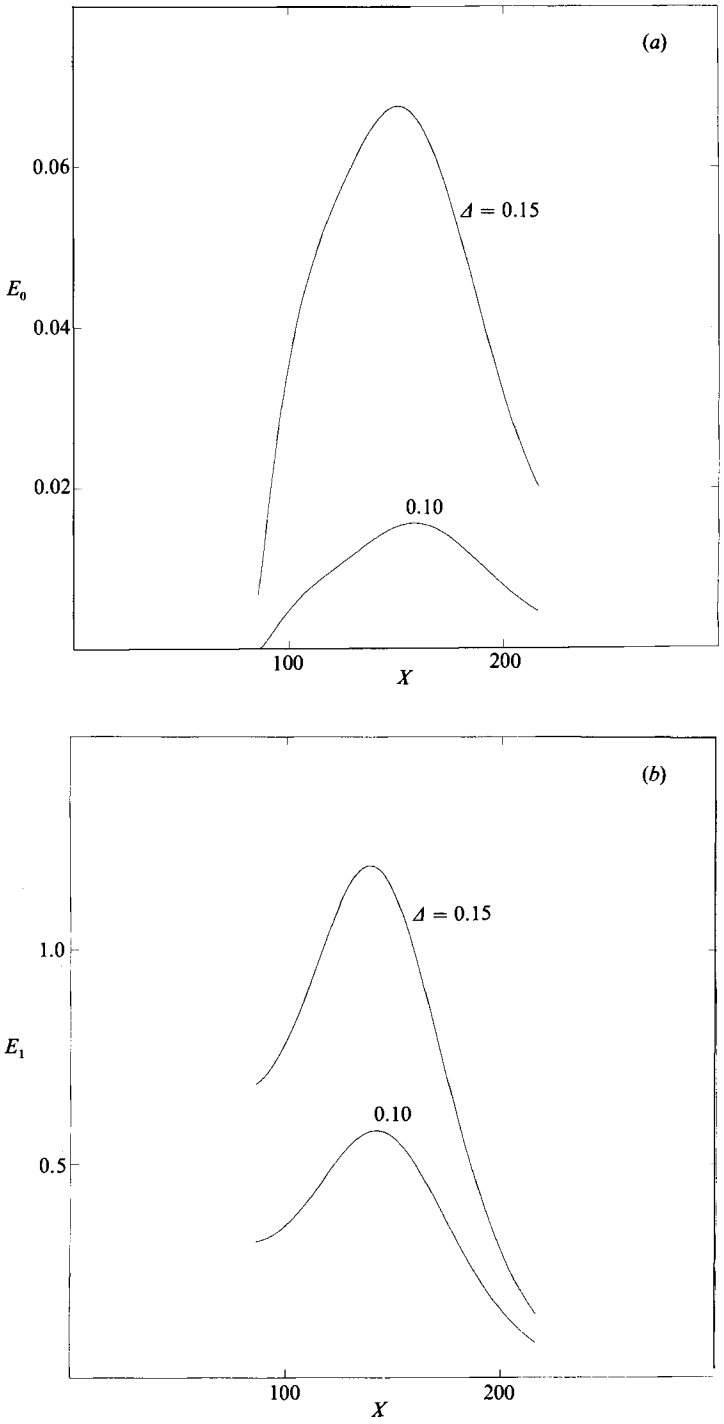

FIGURE 5(*a*, *b*). For caption see facing page.

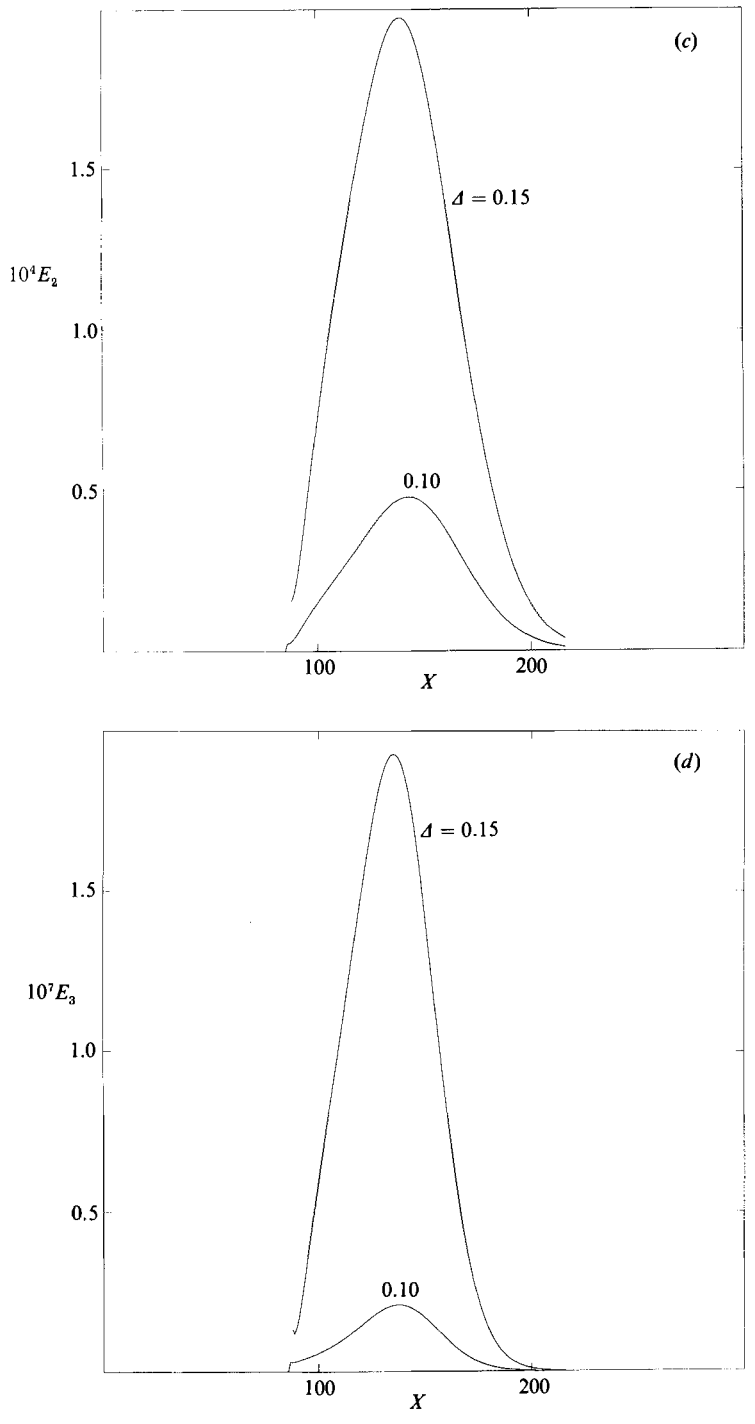

FIGURE 5. The energy function for case (i) with $\Delta = 0.1$, 0.15, $G = 0.1$, $a = 0.16$. (*a*) E_0; (*b*) E_1; (*c*) E_2; (*d*) E_3.

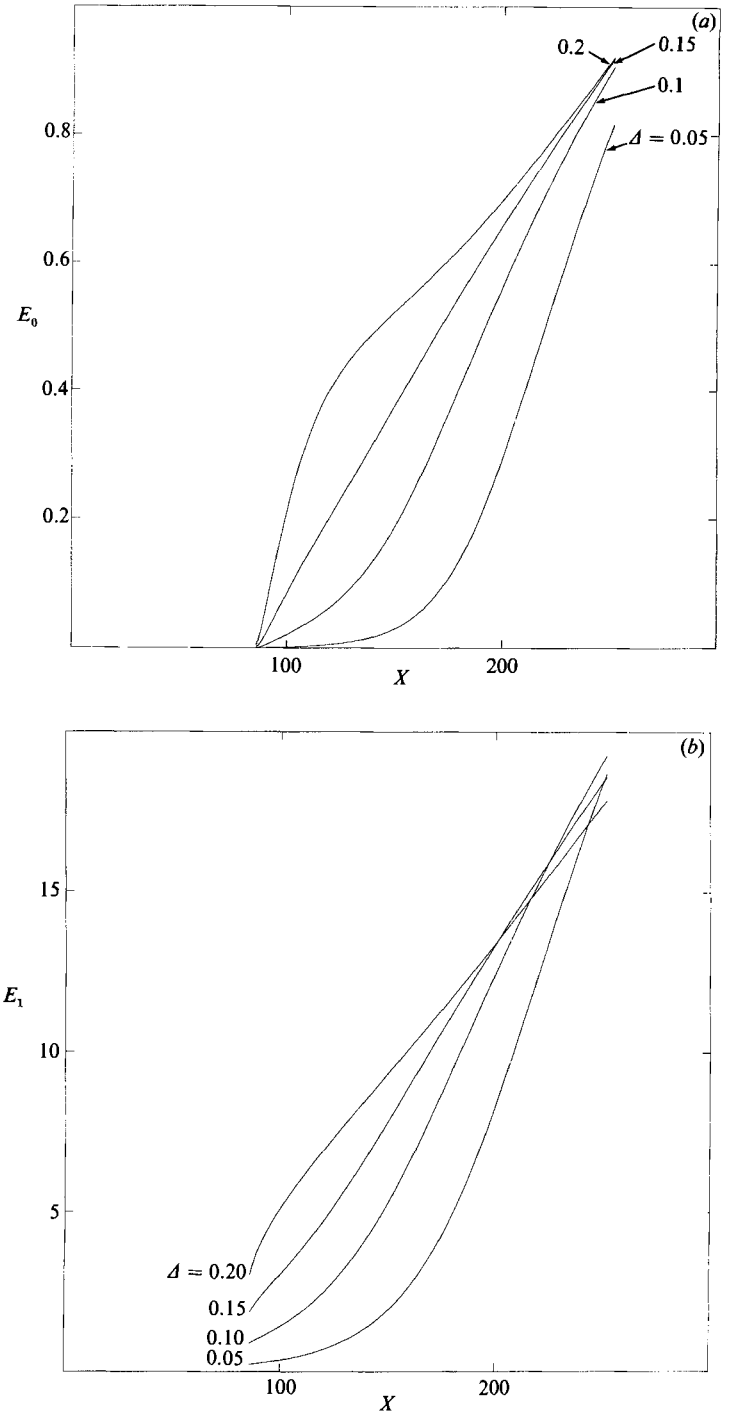

FIGURE 6(*a*, *b*). For caption see facing page.

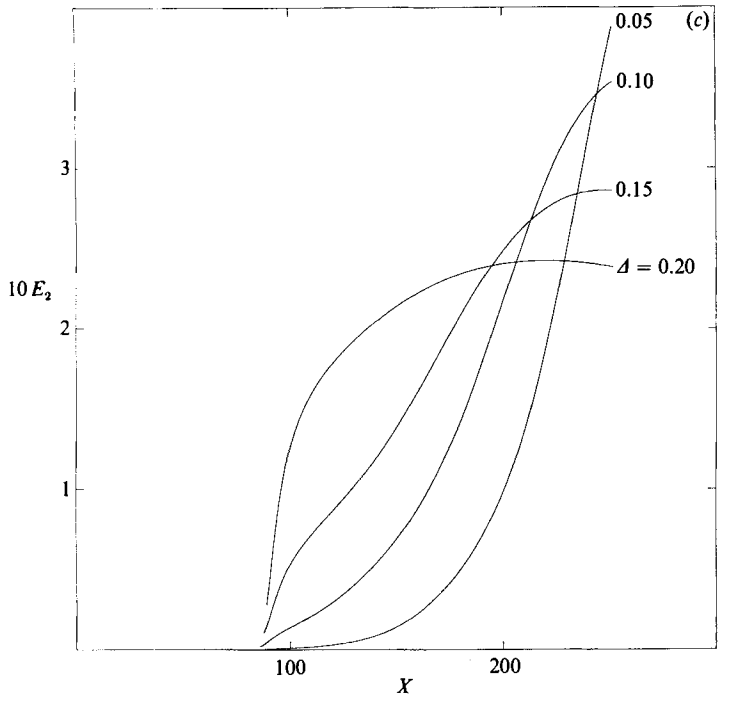

FIGURE 6. The energy function for case (ii) with $\Delta = 0.05, 0.1, 0.15, 0.2$. $G = 0.23$, $a = 0.2$. (*a*) E_0; (*b*) E_1; (*c*) E_2.

calculations were carried out by changing N to 8, ϵ to 0.05 and y_∞ to 100 in turn. The results agreed with those of figure 1 to the graphical accuracy of that figure.

We see in figure 1 that for a 0.5% disturbance the growth rate over the interval shown is indistinguishable from linear theory. At higher values of Δ the growth rate is initially increased above the linear value and then falls below it when X increases. The amount by which the growth rate is decreased from the linear value increases with Δ and we conclude that in this sense nonlinear effects are stabilizing. We attribute the initial increase in the growth rate to the relatively rapid change in flow structure that must necessarily occur when nonlinear effects first become operational.

In figure 2 we have shown the corresponding growth rates for the first harmonic; again we see that after the initial period of decay the disturbance grows when X increases. We note that the growth rates of figures 1 and 2 are comparable even though the first harmonic is locally neutrally stable at a higher Görtler number than is the fundamental. The growth of the first harmonic is of course driven by nonlinear effects. Though the calculations represented in figure 2 clearly indicate the stabilizing effect of nonlinearity, they do not indicate the emergence of any local equilibrium state as the vortices develop downstream.

In figure 3(*a*) we have shown the energy functions E_0 and E_1 corresponding to $\Delta = 0.1, 0.2$ together with $a = 0.2$, $G = 0.0288$ and $\kappa(X) = X/20$. We see that the differences between the values of E_0 and E_1 for $\Delta = 0.1$ and $\Delta = 0.2$ decrease with X. This is presumably because when X is large the effective wavenumber is also large, and the analysis of III suggests that in this regime there exists a unique finite-amplitude solution independent of its initial upstream form. However the calculation of III cannot be applied directly to the calculations reported here since they are

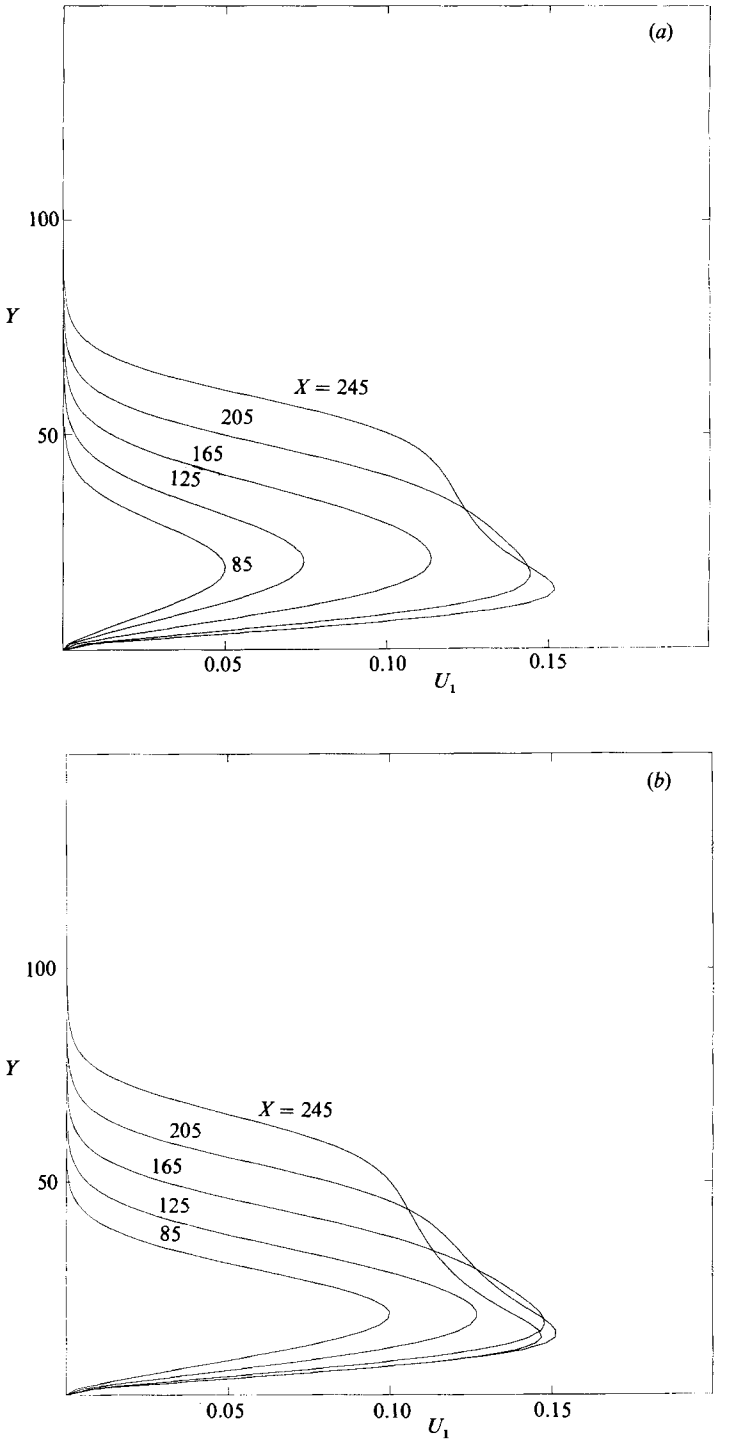

FIGURE 7(*a*, *b*). For caption see page 261.

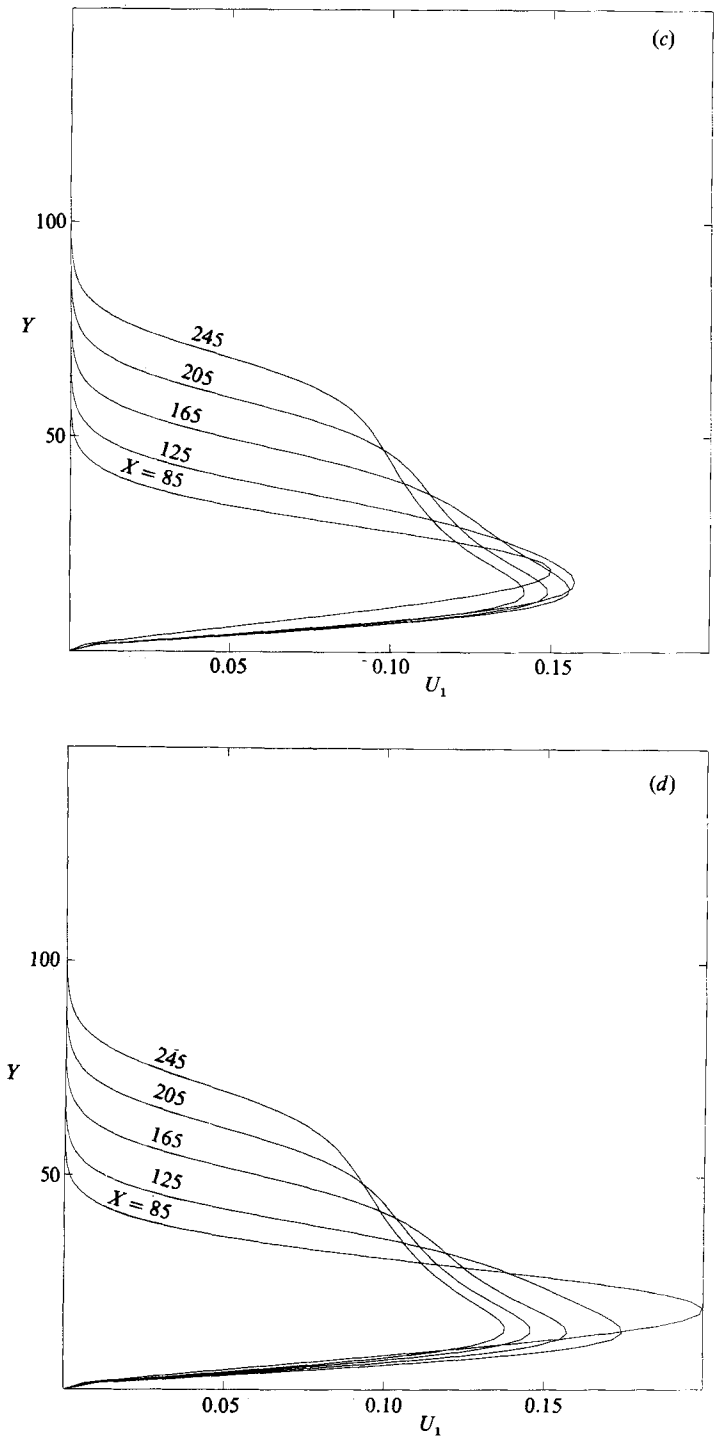

FIGURE 7 (*c*, *d*). For caption see page 261.

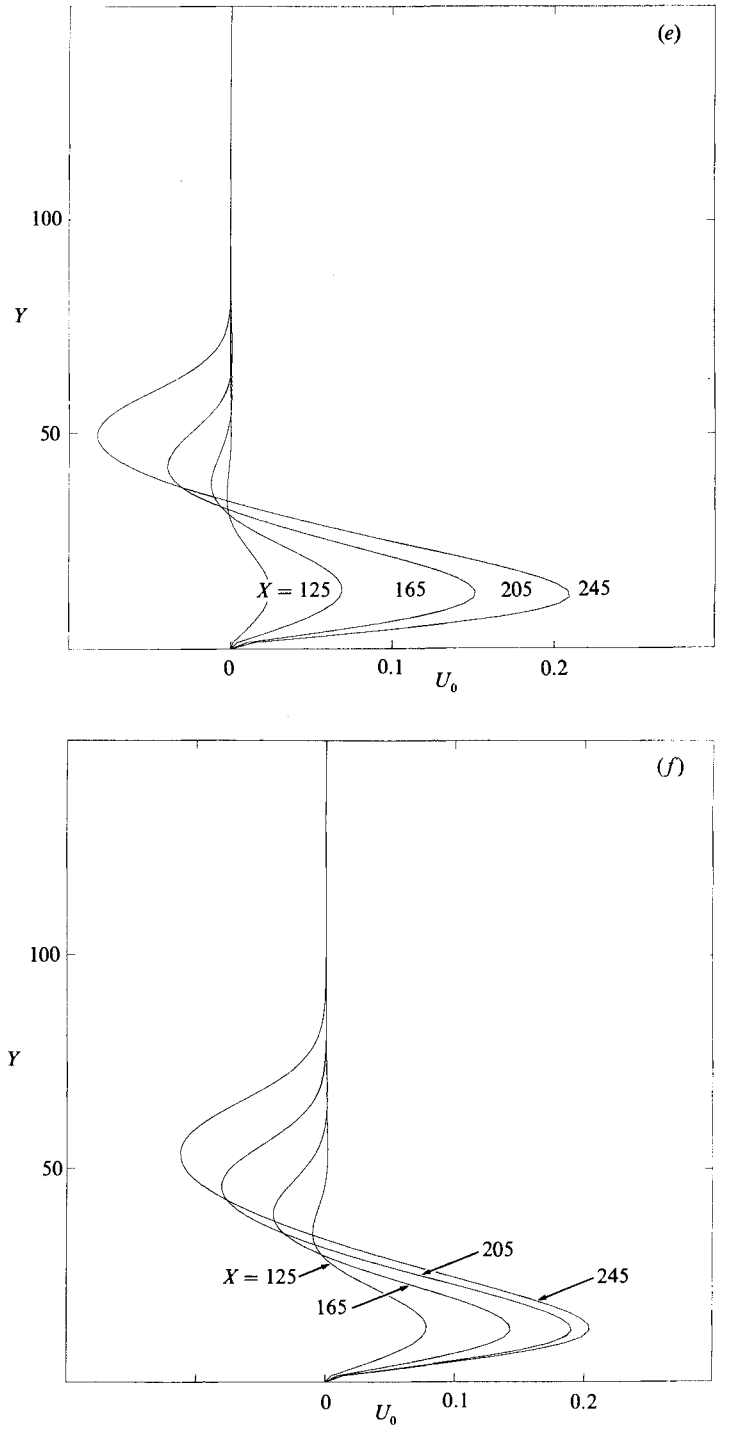

FIGURE 7 (*e*, *f*). For caption see facing page.

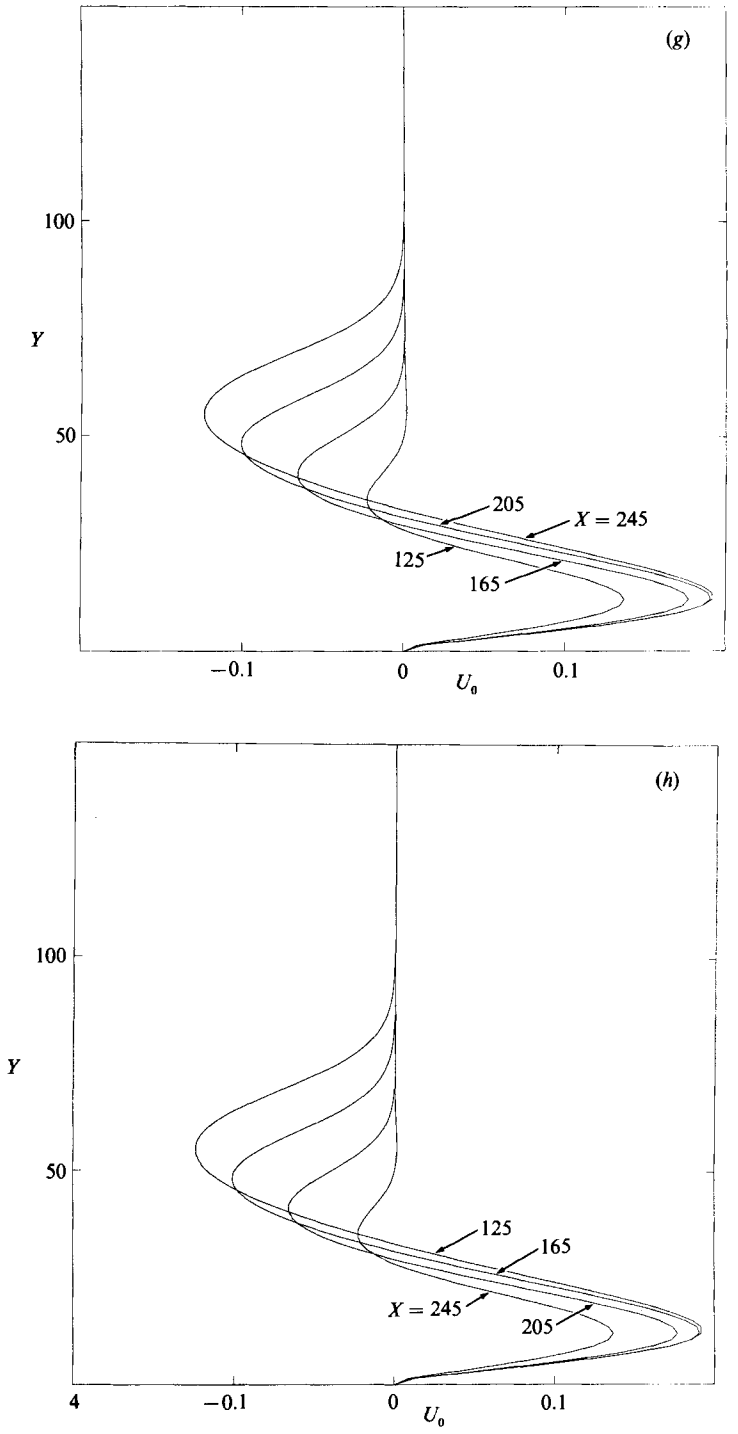

FIGURE 7. (*a–d*) The X velocity component U_1 for case (ii) with $G = 0.23$, $a = 0.2$. (*a*) $\Delta = 0.05$; (*b*) 0.10; (*c*) 0.15; (*d*) 0.20. (*e–h*) The X velocity component U_0 for case (ii) with $G = 0.23$, $a = 0.2$. (*e*) $\Delta = 0.05$; (*f*) 0.10; (*g*) 0.15; (*h*) 0.20.

restricted to an asymptotically small interval near to the neutral location. Nevertheless the short wavelength nonlinear theory of III does suggest that in this regime the origin of the disturbance is unimportant.

In figure 3 (*b*, *c*) we have shown the total downstream velocity component u_T at the spanwise locations $az = \frac{1}{2}\pi, \pi, 2\pi$ together with the Blasius profile which exists in the absence of the vortices. We note that the values of u_T corresponding to $az = \frac{1}{2}\pi$ are identical to those with $az = 3\pi$. The profiles shown correspond to $X = 300$ and we see that at this location there is very little difference between the profiles originating from $A = 0.1$ and $A = 0.2$. Of particular interest is the fact that the $az = \pi$ case has a strongly inflexional profile which, if a parallel-flow stability analysis is applied, is unstable to highly amplified Rayleigh instabilities. The location $az = \pi$ corresponds to the boundary between vortices where the motion of the fluid is away from the wall. We might therefore expect that such locations will be the most susceptible to the secondary instabilities that cause the onset of time dependence in the Görtler problem.

In figure 3 (*d*–*g*) we have shown the individual velocity components appropriate to the above situation with $A = 0.2$. It can be seen that the disturbance is dominated by the fundamental and mean-flow-correction velocity components. We see that, at $X = 300$, U_1 has a significantly different shape than the linear solution initially imposed on the flow at $X = 100$. We have no physical explanation of the nonlinear mechanism that produces this distortion. Before commenting on the experimental relevance of our results we discuss some other calculations performed on walls of different shapes.

Further calculations were carried out for the same initial condition (3.2) but with different curvature distributions $\kappa(X)$. The curvature distributions that we examined in detail and the values of a and G used in the calculations were

$$\text{(i)} \qquad \kappa(X) = \frac{1}{1+(0.02X-2.4)}, \quad a = 0.16, \quad G = 0.1,$$

$$\text{(ii)} \qquad \kappa(X) = \frac{X^{\frac{1}{2}}}{10}, \quad a = 0.2, \quad G = 0.23.$$

The first curvature distribution was chosen because it corresponds to a flow over a hump such that the flow is unstable only over a finite interval. The second distribution was chosen since, as in the asymptotic theory of I, it gives a local Görtler number proportional to the fourth power of the local wavenumber. At relatively large values of X the local growth rate changes little with X and in the nonlinear regime we might expect to recover results qualitatively similar to those of III. The linear growth rate curves corresponding to (i) and (ii) and the initial conditions (3.1) are shown in figure 4.

In figure 5 we have shown the energy functions appropriate to the curvature distribution (i). The linear eigenfunction was obtained by inserting (3.2) at $X = 55$ and integrating until $X = 85$, where the nonlinear terms were turned on. The initial disturbance amplitudes were taken to be $A = 0.1$ and $A = 0.15$. We see that the energy of the disturbance is again almost completely confined to the fundamental and mean flow correction. The maximum value of the disturbance energies E_1, E_2, E_3 occur close to the position where the linear growth rate (i) of figure 4 is zero. In contrast the maximum of E_0 occurs at a higher value of X. This suggests that the results of figure 5 are dominated by the interaction between the basic Blasius

boundary layer and the fundamental component of the disturbance, and never reach any 'local' nonlinear equilibrium state.

In figure 6 the results corresponding to the case (ii) are shown. The nonlinear terms were again turned on at $X = 85$ after integrating (3.2) from $X = 55$, and four calculations corresponding to $\Delta = 0.05, 0.1, 0.15, 0.20$ were carried out. Figure 6 (*a–c*) shows the evolutions with X of the energy function E_0, E_1 and E_2 for this situation. The functions E_0 and E_1 appear to approach limiting forms essentially independent of Δ whilst E_2 initially increases before decaying at sufficiently large values of X. This suggests that as the vortices develop into a region where the effective Görtler number G_x and the effective wavenumber a_x satisfy $G_x \sim a_x^4, a_x \gg 1$ the asymptotic structure found in III is qualitatively recovered. In the latter calculation it was found that small-wavelength Görtler vortices develop through a 'mean-field' interaction between the fundamental and mean flow correction. A quantitative comparison between our results and III is not possible since the asymptotics of III was restricted to an $O(a^{-1})$ neighbourhood of the neutral value of X.

In figure 7 we have shown how U_1 and U_0 vary with X in the above calculations with $\Delta = 0.05, 0.1, 0.15, 0.2$. We see that U_1 in each case for large enough X takes on the characteristic shape found in the calculations for $\kappa \sim X$. Likewise the mean flow correction always evolves into the characteristic shape shown in figure 3 (*g*) for the latter case. We note that the rate at which these shapes are set up increases with the size of the initial perturbations and that the shapes are qualitatively similar to those found in III. Again the fact that the asymptotic solution is valid only very close to the neutral point means that a detailed comparison with III is not possible. The differences between the total downstream velocity component and Blasius flows at different values of X, Z for different values of Δ are shown in figure 8. We can again see the development of a highly inflexional profile at $az = \pi$ which is certainly locally unstable to rapidly growing Rayleigh modes of the type discussed by, for example, Tutty & Cowley (1986). Such a calculation would be formally justified if the wavelength of the Rayleigh instability was small compared to the vortex wavelength. The Rayleigh mode would then be 'trapped' at the spanwise locations where the flow is most unstable on the basis of inviscid theory.

We believe that the major result of our calculations is the demonstration that the nonlinear evolution of streamwise vortices produces inflexional profiles which will presumably break down via a secondary Rayleigh instability. The experiments of, for example, Aihara & Koyama (1981) are consistent with this conclusion and downstream velocity profiles qualitatively similar to ours are presented in this paper. The spanwise locations where the profile is most inflexional in both the experiments and our calculations is at the vortex boundaries where the flow is away from the wall. We note that the shear stress at the wall at these positions is a minimum. Blackwelder (1983) has discussed the possible relationship between the breakdown process of Görtler vortices and the role of streamwise vortices in transition on a flat plate. In the absence of curvature the streamwise vortices could be generated by the interaction of three-dimensional Tollmien–Schlichting waves. Thus it is possible that the streamwise development of local inflexion points which we have observed in our calculations might be relevant to transition in the absence of curvature.

A detailed comparison of our results with experimental observations is not possible since a significant result of the present calculations is that the nature of the initial disturbance effects the downstream evolution of the vortices. We have found that at higher wavenumbers these differences are not so pronounced; unfortunately no

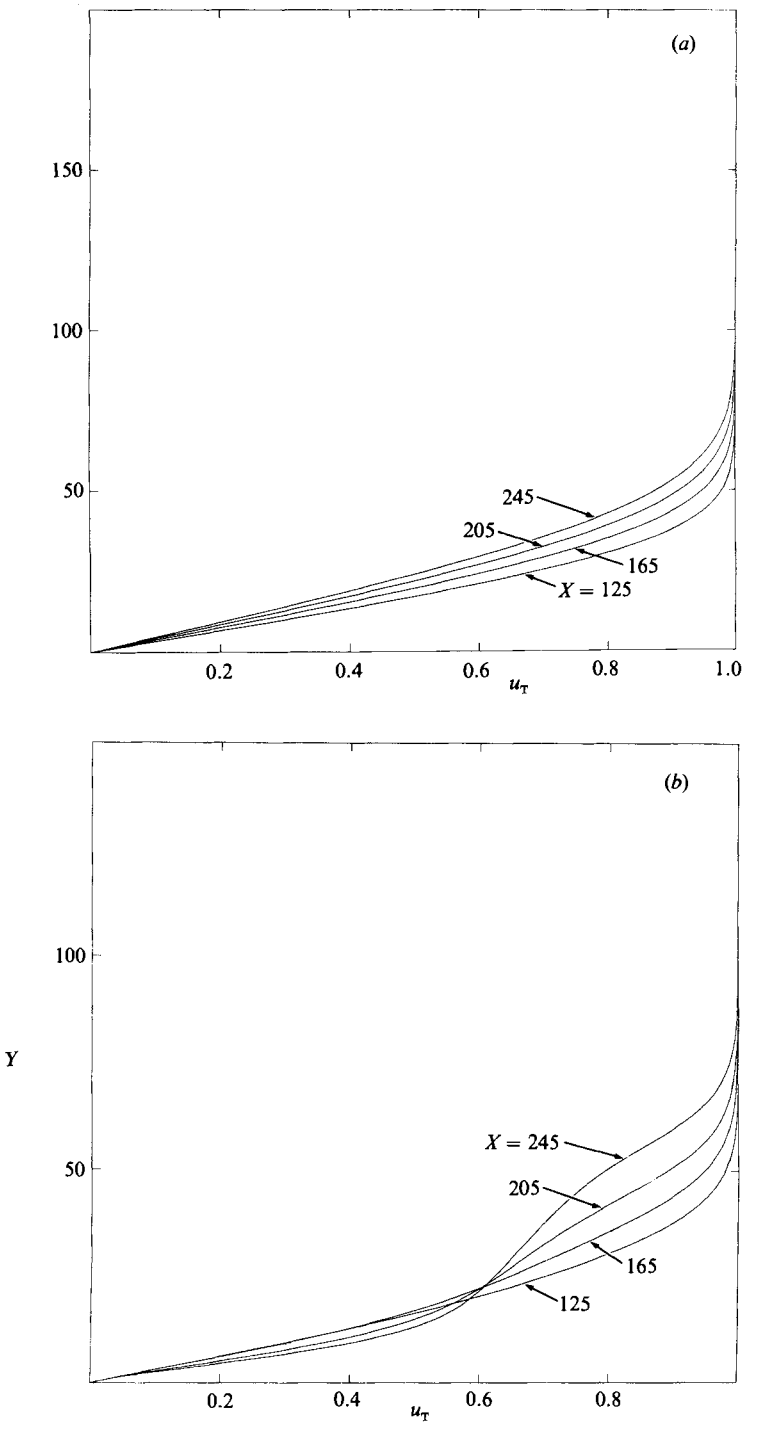

FIGURE 8(*a*, *b*). For caption see facing page.

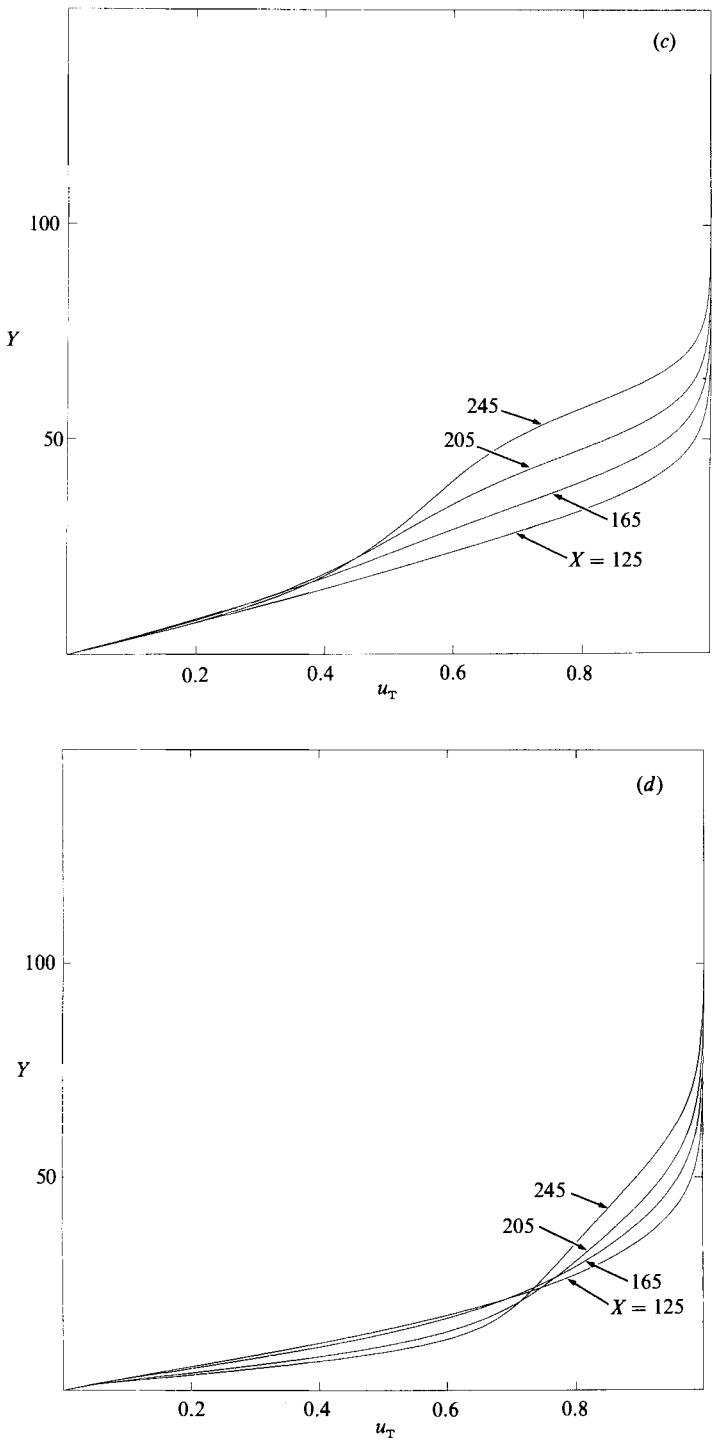

FIGURE 8. (*a*) The total streamwise velocity component for case (ii) with $X = 125$, 165, 205, 245. $G = 0.23$, $a = 0.2$ and (*a*) $\Delta = 0$; (*b*) $\Delta = 0.05$, $az = \frac{1}{2}\pi$; (*c*) $\Delta = 0.05$, $az = \pi$; (*d*) $\Delta = 0.05$, $az = 2\pi$.

experimentally determined profiles have been measured in such a configuration. Thus the most we can say is that our results are qualitatively similar to the few experimentally determined profiles that have been published.

This work was carried out whilst the author was at ICASE, NASA Langley. Supported by NSAI-17070.

REFERENCES

AIHARA, Y. 1976 Nonlinear analysis of Görtler vortices. *Phys. Fluids* **19**, 1655.

AIHARA, Y. & KOYAMA, H. 1981 Secondary instability of Görtler vortices: Formation of periodic three-dimensional coherent structure. *Trans. Japan Soc. Aero Space Sci.* **24**, 78.

BENNETT, J. & HALL, P. 1988 On the secondary instability of Taylor–Görtler vortices to Tollmien–Schlichting waves in fully developed flows. *J. Fluid Mech.* **186**, 445–469.

BLACKWELDER, R. 1983 Analogies between transitional and turbulent boundary layers. *Phys. Fluids* **26**, 2807.

FLORYAN, J. & SARIC, W. S. 1979 Stability of Görtler vortices in boundary layers. *AIAA paper* 79-1497.

GÖRTLER, H. 1940 Über eine dreidimensionale Instabilität laminarer Grenzschichten an Konkaven Wänden. *Nachr. Acad. Wiss. Göttingen Math. Phys.* **K1. 2**, No. 1.

GREGORY, N., STUART, J. T. & WALKER, W. S. 1955 On the stability of three-dimensional boundary layers with application to the flow over a rotating disc. *Phil. Trans. R. Soc. Lond.* A **248**, 155.

HALL, P. 1982*a* Taylor–Görtler instabilities in fully developed or boundary layer flows: linear theory. *J. Fluid Mech.* **124**, 475.

HALL, P. 1982*b* On the nonlinear evolution of Görtler vortices in growing boundary layers. *J. Inst. Maths Applics.* **29**, 173.

HALL, P. 1983 The linear development of Görtler vortices in growing boundary layers. *J. Fluid Mech.* **130**, 41.

HÄMMERLIN, G. 1956 Zur Theorie der dreidimensionalen Instabilitat laminar Grenschichten. *Z. Angew. Math. Phys.* **1**, 156.

HERBERT, T. 1976 On the stability of a boundary layer on a curved wall. *Arch. Mech.* **28**, 1039.

SMITH, A. M. O. 1955 On the growth of Taylor–Görtler vortices along highly concave walls. *Q. Appl. Maths.* **13**, 233.

TUTTY, O. R. & COWLEY, S. J. 1986 On the stability and numerical solution of the unsteady boundary layer equations. *J. Fluid Mech.* **168**, 431.